The Journal of Neuroscience, June 1, 1997, 17(11):4180–4189

Reduction of CuZn-Superoxide Dismutase Activity Exacerbates Neuronal Cell Injury and Edema Formation after Transient Focal Cerebral Ischemia

Takeo Kondo,[1,2] Andrew G. Reaume,[4] Ting-Ting Huang,[3] Elaine Carlson,[3] Kensuke Murakami,[1,2] Sylvia F. Chen,[1,2] Eric K. Hoffman,[4] Richard W. Scott,[4] Charles J. Epstein,[3] and Pak H. Chan[1,2]

Departments of [1]Neurological Surgery, [2]Neurology, and [3]Pediatrics, University of California School of Medicine, San Francisco, California 94143, and [4]Department of Molecular Biology, Cephalon, Incorporated, West Chester, Pennsylvania 19380

Apoptotic neuronal cell death has recently been associated with the development of infarction after cerebral ischemia. In a variety of studies, CuZn-superoxide dismutase (CuZn-SOD) has been shown to protect the brain from ischemic injury. A possible role for CuZn-SOD-related modulation of neuronal viability is suggested by the finding that CuZn-SOD inhibits apoptotic neuronal cell death in response to some forms of cellular damage. We evaluated this possibility in the model of transient focal cerebral ischemia in mice bearing a disruption of the CuZn-SOD gene (*Sod1*). Homozygous mutant (*Sod1* −/−) mice had no detectable CuZn-SOD activity, and heterozygous mutants (*Sod1* +/−) showed a 50% decrease compared with wild-type mice. *Sod1* −/− mice showed a high level of blood–brain barrier disruption soon after 1 hr of middle cerebral artery occlusion and 100% mortality at 24 hr after ischemia. *Sod1* +/− mice showed 30% mortality at 24 hr after ischemia, and neurological deficits were exacerbated compared with wild-type controls. The *Sod1* +/− animals also had increased infarct volume and brain swelling, accompanied by increased apoptotic neuronal cell death as indicated by the *in situ* nick-end labeling technique to detect DNA fragmentation and morphological criteria. These results suggest that oxygen-free radicals, especially superoxide anions, are an important factor for the development of infarction by brain edema formation and apoptotic neuronal cell death after focal cerebral ischemia and reperfusion.

Key words: CuZn-superoxide dismutase; focal cerebral ischemia; blood–brain barrier; Evans blue extravasation; neuronal apoptosis; TUNEL; oxidative stress

Oxygen-free radicals are believed to be involved in the pathogenesis after cerebral ischemia and reperfusion. During cerebral ischemia, a number of events that predispose the brain to the formation of oxygen-free radicals may occur (Siesjö, 1984; McCord, 1985). After reperfusion, these events can set off a cascade of other biochemical and molecular sequelae such as the xanthine–xanthine oxidase reaction and phospholipase activation, leading to free-radical production (Gaudet and Levine, 1979; Chan et al., 1984; Siesjö, 1984; McCord, 1985). Among these oxygen-free radicals, superoxide anion (O_2^-), being directly toxic to neurons (Fridovich, 1986; Patel et al., 1996), may initiate a free radical-mediated chain reaction causing additional CNS damage (Saugstad and Aasen, 1980; Chan, 1994).

One of the manifestations of CNS damage after cerebral ischemia is the formation of brain edema caused by the breakdown of the blood–brain barrier (BBB). CuZn-superoxide dismutase (CuZn-SOD), a cytosolic protein, prevents vasogenic brain edema after several kinds of injuries (Chan et al., 1991; Kinouchi et al., 1991; Shukla et al., 1993), suggesting that O_2^- is an important factor for BBB disruption. Another manifestation of CNS damage is the direct injury of neuronal cells, including excitatory events that are induced by glutamate release after cerebral ischemia. Glutamate elevates cytosolic free calcium (Ca^{2+}) (Choi, 1988), which activates Ca^{2+}-dependent enzymes and leads to free radical production (Orrenius et al., 1992; Pazdernik et al., 1992). Recent studies suggest that excitotoxic injury causes apoptotic neuronal cell death in some neuronal subpopulations (Kure et al., 1991; Ankarcrona et al., 1995). Both CuZn-SOD (Greenlund et al., 1995) and BCL-2, which recently has been shown to have an antioxidant property (Kane et al., 1993), inhibit apoptotic neuronal cell death, suggesting the possibility that oxygen-free radicals may modulate neuronal apoptosis. Apoptotic neuronal cell death may also play an important role in focal ischemic brain injury (Linnik et al., 1993; Tominaga et al., 1993; MacManus et al., 1994; Li et al., 1995b).

The development of mice deficient in the mouse CuZn-SOD gene (*Sod1*) has provided a model for assessing the role of CuZn-SOD in nervous system injuries (Reaume et al., 1996) (T. Huang, M. Yasunami, E. Carlson, A. Gillespie, A. Reaume, E. Hoffman, P. Chan, R. Scott, C. Epstein, unpublished data). These mutant mice with a decrease in or complete absence of endogenous CuZn-SOD activity do not show any phenotypic abnormalities under normal physiological conditions. However, we hypothesized that the mutant mice might be vulnerable to oxidative stress because of additional oxygen-free radical formation after ischemia and reperfusion. Using an *in vivo* model of focal cerebral ischemia and reperfusion, we now show early BBB disruption and

Received Jan. 30, 1997; revised March 17, 1997; accepted March 21, 1997.

This work was supported by National Institutes of Health Grants NS14543 and NS25372 (P.H.C.) and AG08938 (C.J.E., P.H.C.), and by the Lucille Markey Foundation to the University of California, San Francisco, Program in Biological Sciences. We thank L. F. Reola and B. E. Calagui for their expert technical assistance and C. Christensen for her editorial assistance. We particularly thank F. R. Sharp, J. Honkaniemi, K. Lamborn, and H. Kinouchi for their suggestions.

Correspondence should be addressed to Dr. P.H. Chan, Departments of Neurological Surgery and Neurology, University of California, Box 0651, San Francisco, CA 94143.

high mortality in the mutant mice with reduced CuZn-SOD activity. In addition, using an *in situ* technique to detect the DNA free 3′-OH ends, we have found that apoptotic neuronal cell death is increased in the mutant mice after ischemia and reperfusion. These data indicate that oxygen-free radicals, especially O_2^-, are important mediators of brain edema and apoptotic neuronal cell death in focal ischemic brain injury.

MATERIALS AND METHODS

Sod1-*deficient mice.* In the present study, we used two independent sources of mutant mice. One strain of mutant mice designated 129/CD1-*Sod1*<tm1 Cep> was produced at Cephalon (West Chester, PA) (Reaume et al., 1996). This mutant was made by targeted deletion of the *Sod1* gene in embryonic stem (ES) cells using a positive-negative selection scheme that replaced all *Sod1* coding sequences (7.6 kb) with the neomycin resistance gene. The mutant ES cells were in turn used to create mice that were either heterozygous (*Sod1* $+/-^{cep}$) or homozygous (*Sod1* $-/-^{cep}$) mutants. Another strain of mutant mice designated CD1-*Sod1*<tm1 Cje> was produced in the Department of Pediatrics, University of California, San Francisco (T.-T. Huang et al., unpublished data). This mutant was made by targeted deletion of the *Sod1* gene in ES cells using an alternative positive-negative selection scheme that replaced a portion of exon 3 and the entire exon 4 of the *Sod1* gene (1.9 kb) with the neomycin resistance gene. The mutant ES cells were in turn used to create mice that were heterozygous (*Sod1* $+/-^{uc}$) mutants. All these mutant mice were bred with the CD1 strain of mice. In the present study, age-matched wild-type (Wt) 129/CD1 mice were used as controls.

Two methods were used for assessing of CuZn-SOD activity in the mutant mice. For the gel electrophoresis assay, previously described methods (Epstein et al., 1987) were used. For the measurement of CuZn-SOD-specific activity, supernatant fluids from red blood cell lysates or brain homogenates were assayed by a previously described method based on cytochrome C reduction (McCord and Fridovich, 1969). CuZn-SOD activity, which reduces the cytochrome C deoxidative capacity by half, was taken as one unit. Tissue protein was quantified using BCA protein assay reagent (Pierce, Rockford, IL), and CuZn-SOD activity was calculated in relation to the mass of protein.

Focal cerebral ischemia and neurological assessment. Focal cerebral ischemia was achieved with suture monofilament blockade of the middle cerebral artery (MCA) using the previously described method of Yang et al. (1994), with some modification. Male 2- to 3-month-old Wt or mutant mice (35–40 gm) were anesthetized with 1.5% isoflurane in a 30% O_2/70% N_2O mixture under spontaneous breathing. The rectal temperature was controlled at 37.0 ± 0.5°C during surgery with a feedback regulated heating pad. After exposing the left carotid artery, a 5–0 Dermalon suture (1756-41, Devis and Geck, Manati, Puerto Rico) was advanced into the internal carotid artery 12 mm from the lumen of the external carotid artery. The ipsilateral common carotid artery was occluded with a small surgical clip immediately after suture blockade. The animals underwent MCA occlusion for 1 hr and were then subjected to reperfusion by removing the suture and the clip. Mean arterial blood pressure and cerebral blood flow (CBF) were monitored as physiological parameters during ischemia, and arterial blood gas was analyzed after reperfusion. After recovering from anesthesia, the animals were maintained in an air conditioned room at 20°C during the reperfusion periods (2–96 hr).

At 24 hr after 1 hr of MCA occlusion, surviving mice were evaluated by a blinded observer for their neurological deficits. The neurological deficit score assignment of 0 to 4 was based on the methods described previously by Yang et al. (1994). After evaluating the scores, the brains were removed and rapidly frozen and then were analyzed histologically with cresyl violet staining. Animals that had massive hematomas in the brain or no infarction in the brain were omitted from the neurological analysis.

Measurement of Evans blue extravasation. A quantitative assay of Evans blue was based on the method described previously by Chan et al. (1991). Just after reperfusion, 0.1 ml of 4% Evans blue (Sigma, St. Louis, MO) in 0.9% saline was intravenously injected. At 2, 8, or 24 hr after the injection, the animals were killed by transcardiac perfusion using 200 ml of heparinized saline (10 U/ml heparin in 0.9% of saline), and the brains were removed. After removing the cerebellum and brainstem, the cerebral hemispheres were separated into the ischemic hemispheres and nonischemic hemispheres. Each hemisphere was well homogenized in 1 ml of 0.1 M PBS. After 1000 × *g* spin for 5 min, 0.7 ml of supernatant was taken, and 0.7 ml of 100% (w/v) trichloroacetic acid was added. The mixture was incubated at 4°C for 18 hr, then centrifuged at 1000 × *g* for 30 min. The Evans blue concentration of the supernatant was measured at 610 nm by a spectrophotometer. Results are presented as milligrams of Evans blue/hemisphere by comparing it with the standard solution.

Histological analysis. At 8, 24, 48, or 96 hr after 1 hr of MCA occlusion, the brains were removed and frozen rapidly. The brains were sectioned with a cryostat into a 20 μm thickness from the anterior side to the posterior side at 500 μm intervals. The sections were stained with cresyl violet using standard histological criteria. The staining image was scanned by Color One Scanner 600/27 (Apple Computer, Cupertino, CA) at 1200 dpi resolution. The infarct area and the bilateral hemispheric area were measured by the National Institutes of Health system in 14 sections from the anterior tip of the brain. The total infarct volume and total hemispheric volume were calculated according to the method of Liu et al. (1989).

In situ *labeling of DNA fragmentation.* At 8, 24, 48, or 96 hr after 1 hr of MCA occlusion, the brain sections at the level of the caudate putamen that show typical infarction were stained using an *in situ* technique to detect the DNA free 3′-OH ends (TUNEL) reaction (Gavrieli et al., 1992). Frozen brain sections were fixed for 30 min in 4% formaldehyde in 0.1 M PBS, pH 7.4. The slides were placed in 1 × terminal deoxynucleotidyl transferase buffer (Life Technologies, Gaithersburg, MD) for 15 min, followed by 10 μl/ml of terminal deoxynucleotidyl transferase enzyme (Life Technologies) with 40 μl/ml biotinylated 16-dUTP (Boehringer Mannheim, Indianapolis, IN) at 37°C for 60 min. The slides were then washed in 2× SSC (150 mM sodium chloride, 15 mM sodium citrate, pH 7.4) for 15 min, followed by PBS two times for 15 min. Avidin–biotin horseradish peroxidase solution (ABC kit, Vector Laboratories, Burlingame, CA) was applied to the sections for 30 min, then washed with PBS two times for 15 min. Staining was visualized using 0.025% diaminobenzidine and 0.075% H_2O_2 in PBS. After staining, the slides were rinsed with water. Slides were then stained with methyl green for 10 min and dehydrated and mounted. Slides were observed with either a bright-field or a dark-field phase-contrast microscopy (Diaphot-TMD, Nicon, Tokyo, Japan). In the latter, a yellow filter, which is used for detection of fluorescent isothiocyanate, was used without excitation. Consecutive sections were stained with hematoxylin and eosin (H & E) to observe standard morphological criteria.

Cell counts. A blinded observer counted the number of TUNEL-positive cells in 625 μm^2 pixels in 400× magnification of light-field microgram. Positive cells were determined carefully by the criteria described by Charriaut-Marlangue and Ben-Ari (1995) and counted in 200 pixels (0.125 mm^2) with random movement under blinded conditions to avoid intentional selection. Individual regions were determined as follows: inner boundary of the caudate putamen from the medial edge of the infarction to 200 μm toward infarct area; center of the caudate putamen from external capsule to 500 μm toward midline; cortical penumbra from the edge of the infarction to 1 mm toward infarct area; the piriform cortex inside of the piriform cortex neuronal cell layer. The total positive cell number in 200 pixels was expressed as cells/mm^2.

Statistical analysis. All measurements, except the neurological deficit score, were statistically analyzed using one-way ANOVA followed by Fisher's protected least-significant difference (PLSD) test. The neurological deficit score was analyzed statistically using a nonparametric test (Kruskal–Wallis test for overall effects, followed by the Mann–Whitney *U* test for individual group comparisons). Spearman rank correlation followed by linear regression analysis was used for correlation study.

RESULTS

CuZn-SOD activity and physiological parameters in mutant mice

Nondenatured gel electrophoresis followed by nitroblue tetrazolium staining confirms that CuZn-SOD activity is reduced in both *Sod1* $+/-^{uc}$ and *Sod1* $+/-^{cep}$ and completely absent in *Sod1* $-/-^{cep}$ (Fig. 1). A quantitative assay of CuZn-SOD activity shows ~50% reduction in both *Sod1* $+/-^{uc}$ and *Sod1* $+/-^{cep}$ and only a trace of activity in *Sod1* $-/-^{cep}$ (Table 1). Although the gene-targeted locus is different in the two independent lines of heterozygous mutant mice (*Sod1* $+/-^{uc}$ and *Sod1* $+/-^{cep}$), these mice show the same level of CuZn-SOD activity. The minor level of activity in *Sod1* $-/-^{cep}$ likely represents background from the

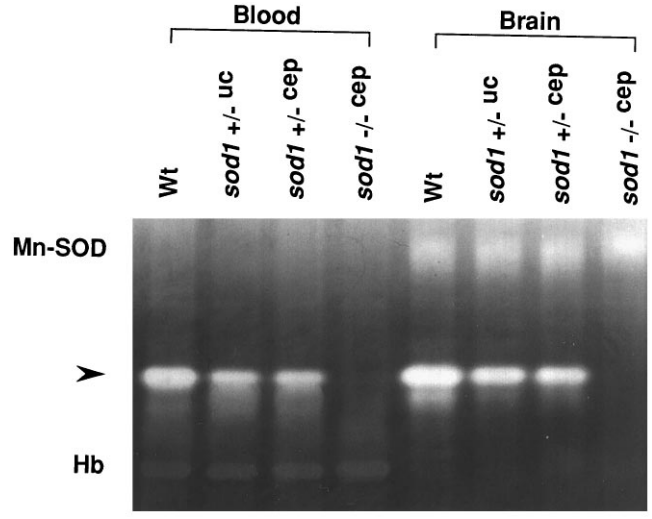

Figure 1. CuZn-SOD activity in mutant mice. CuZn-SOD activity analysis of blood (*lanes 1-4*) and brain tissue homogenate (*lanes 5-8*). Nondenatured gel electrophoresis followed by nitroblue tetrazolium staining shows a white band (*arrowhead*), corresponding to CuZn-SOD activity. There are also visible bands, corresponding to manganese (*Mn*)-SOD and hemoglobin (*Hb*). *Lanes 1* and *5*, Wt; *2* and *6*, *Sod1* $+/-^{uc}$; *3* and *7*, *Sod1* $+/-^{cep}$; *4* and *8*, *Sod1* $-/-^{cep}$.

Table 1. Quantitative analysis of CuZn-SOD activity in Wt and mutant mice

Genotype	CuZn-SOD Activity (%) Blood (n = 9)	Brain (n = 3)
Wt	100	100
Sod1 $+/-^{uc}$	53.1 ± 1.1	52.2 ± 2.3
Sod1 $+/-^{cep}$	61.6 ± 5.8	47.7 ± 4.6
Sod1 $-/-^{cep}$	5.4 ± 7.5	6.6 ± 7.6

CuZn-SOD activity was measured by a method based on cytochrome C reduction (McCord and Fridovich, 1969). Each value represents mean ± SEM of the percentages of CuZn-SOD activity, compared with Wt.

assay, although it also could reflect an endogenous SOD activity contributed by the extracellular form of CuZn-SOD that exists in the brain and plasma. Physiological studies show no significant differences in arterial blood gas analysis, middle arterial blood pressure, or CBF between Wt and all mutant mice (Table 2).

Mortality and neurological deficits are exacerbated in mutant mice

The mortality of Wt and mutant animals during 24 hr after 1 hr of MCA occlusion is shown in Table 3. All *Sod1* $-/-^{cep}$ mice were dead within several hours after ischemia, and the rate of mortality was significantly higher than that of Wt mice ($p < 0.01$) (Table 3). Although the rate of mortality was moderately higher in both *Sod1* $+/-^{uc}$ and *Sod1* $+/-^{cep}$ than in Wt mice at 24 hr, no significance was seen (Table 3). However, the mortality was significantly higher for *Sod1* +/− animals at 48 and 96 hr after ischemia, compared with Wt mice. In surviving animals, neurological deficits were exacerbated significantly in *Sod1* $+/-^{uc}$ and *Sod1* $+/-^{cep}$ mice, compared with Wt mice at 24 hr ($p < 0.05$–0.01) (Table 4).

Evans blue extravasation indicates the early BBB disruption in mutant mice

At 2 hr after 1 hr of MCA occlusion, no Evans blue leakage occurred in the entire brain of Wt mice, including the ischemic region (Fig. 2*A*). In contrast, *Sod1* +/− mice showed a minor level of Evans blue extravasation around the center of the ischemic region (Fig. 2*A*). The Evans blue extravasation was much more intensified and extended to the entire ischemic region in the *Sod1* −/− mice (Fig. 2*A*).

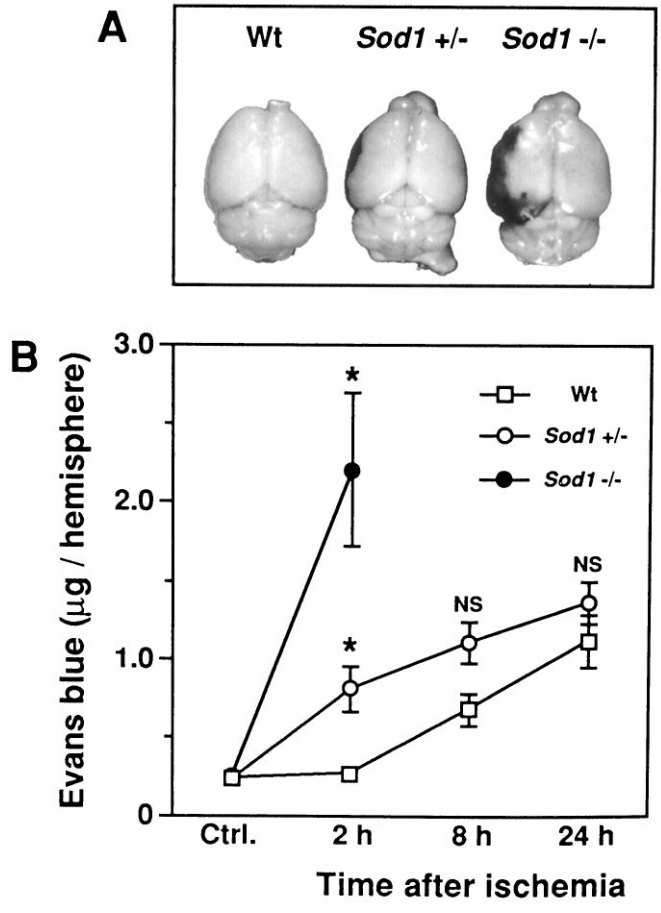

Figure 2. Evans blue extravasation in mutant mice after ischemia. *A*, Representative photographs of Evans blue extravasation in the brains of Wt mice, heterozygous (*Sod1* +/−) and homozygous (*Sod1* −/−) mutants 2 hr after ischemia. The dark stained area in the left hemisphere indicates Evans blue extravasation. *B*, Quantitative assay of Evans blue at 2, 8, or 24 hr after ischemia. Values are mean ± SEM of the amount of Evans blue in the hemisphere. *Ctrl.*, Basal value of Evans blue in the nonischemic hemisphere of Wt (n = 16), *Sod1* +/− (n = 19), or *Sod1* −/− (n = 5) mice. Data in respective time points indicate the amount of Evans blue in the ischemic hemisphere of Wt, *Sod1* +/−, or *Sod1* −/− mice (n = 4–8). *Asterisks* indicate a significant increase of Evans blue leakage compared with Wt mice ($p < 0.01$), and *NS* indicates no significance between Wt and *Sod1* +/− (Fisher's PLSD test).

As illustrated in Figure 2*B*, quantitative assay of Evans blue revealed a low background basal level of Evans blue extravasation in the nonischemic hemisphere: Wt, 0.23 ± 0.02; *Sod1* +/−, 0.22 ± 0.01; *Sod1* −/−, 0.24 ± 0.05 (mean ± SEM of μg/hemisphere; no significant difference in any of the groups, by ANOVA). At 2 hr after 1 hr of MCA occlusion, the amount of Evans blue leakage was not increased in the ischemic hemisphere of the Wt mice (0.26 ± 0.02 μg/hemisphere), although it was moderately increased in the ischemic hemisphere of *Sod1* +/− (0.81 ± 0.15 μg/hemisphere; $p < 0.01$) (Fig. 2*B*) and was highly increased in the ischemic hemisphere of *Sod1* −/− (2.21 ± 0.49 μg/hemisphere; $p < 0.01$) (Fig. 2*B*). Evans blue leakage in-

Table 2. Physiological parameters of Wt and mutant mice during and after ischemia

Genotype	Arterial blood gas analysis			MABP (mmHg)	Residual CBF (%)[a]
	pH	pCO_2 (torr)	pO_2 (torr)		
Wt	7.30 ± 0.02	42.7 ± 1.2	151.9 ± 13.8	83.0 ± 4.7	12.4 ± 2.7
Sod1+/−^{uc}	7.32 ± 0.06	34.8 ± 3.0	181.6 ± 8.2	88.0 ± 4.0	13.9 ± 3.2
Sod1+/−^{cep}	7.30 ± 0.02	41.6 ± 2.4	138.5 ± 4.8	90.0 ± 2.1	11.4 ± 4.6
Sod1−/−^{cep}	7.32 ± 0.03	35.2 ± 3.0	165.4 ± 6.9	89.0 ± 6.0	13.3 ± 1.1

Each value represents mean ± SEM ($n = 4$).

[a]CBF was measured by laser Doppler flowmetry according to the method of Kamii et al. (1994) and represented by the percentage of residual value, calculated as (CBF during ischemia/CBF before ischemia) × 100%.

creased in Wt mice at 8 hr after ischemia and gradually increased up to 24 hr (Fig. 2*B*). Also, *Sod1* +/− mice showed an increasing amount of Evans blue extravasation up to 24 hr, although no significant difference was seen, compared with Wt at 8 and 24 hr after ischemia (Fig. 2*B*). No Evans blue leakage studies were performed in *Sod 1* −/− mice at 8 and 24 hr because of 100% animal mortality. These results suggest that a decreased level of CuZn-SOD activity in the mutant mice mediates early BBB breakdown after cerebral ischemia.

Infarct volume and brain swelling are exacerbated in mutant mice

To investigate the correlation between the degree of ischemic infarction and CuZn-SOD activity, we compared the infarct size between Wt and heterozygous mutant mice after 1 hr of MCA occlusion. Hemisphere enlargement was also measured to evaluate the brain swelling contributed by brain edema. As shown in Figure 3*A*, the infarct area and the normal area can be clearly defined by cresyl violet staining. Distribution of the infarction and brain swelling at 24 hr after ischemia are shown in Figure 3*B*. Distribution of the infarction is similar in the two different strains of mutants (*Sod1* +/−^{uc} and *Sod1* +/−^{cep}), which is remarkably extended to the posterior side of the brain, compared with that of Wt mice (Fig. 3B_1). The hippocampal CA1 pyramidal neurons, especially, which were spared in Wt mice, are involved in the infarction in the heterozygous mutant mice (Fig. 3*A*). In contrast, the percentage of hemisphere enlargement was continuously greater in all of the brain sections in both of the heterozygous mutants (*Sod1* +/−^{uc} and *Sod1* +/−^{cep}) than in the Wt mice (Fig. 3B_2).

Next we assessed the total infarct volume and hemisphere enlargement in the whole brain by calculating the cumulative areas in consecutive brain sections at 8, 24, 48, and 96 hr after ischemia. As illustrated in Figure 3C_1, infarction was not obvious at 8 hr after ischemia, except in the lateral caudate putamen (i.e., core of the ischemia), both in Wt and *Sod1* +/−^{cep} mice (4.2 ± 0.3% vs 7.1 ± 0.5%; $p = 0.68$). The infarct volume was increased at 24 hr after ischemia and was significantly greater in *Sod1* +/−^{cep} (53.0 ± 5.5%) than in Wt mice (28.4 ± 3.4%; $p < 0.01$) (Fig. 3C_1). The infarct volume remained at 48 hr after ischemia both in Wt and in *Sod1* +/−^{cep} mice (33.1 ± 3.3% vs 55.0 ± 6.1) ($p < 0.01$) (Fig. 3C_1). Although the infarct volume was reduced slightly at 96 hr after ischemia in *Sod1* +/−^{cep} mice (47.7 ± 3.3%), it was still significantly greater than in Wt mice (32.2 ± 3.5%; $p < 0.05$) (Fig. 3C_1). One possibility to explain the unlikely phenomenon of the reduction of infarct volume in temporal resolution is the high mortality in *Sod1* +/−^{cep} mice, as demonstrated in Table 3. The mortality rates of the *Sod1* +/− animals were 50 and 63.6% for 48 and 96 hr, whereas the mortality rates of Wt mice were 28.6 and 55.6%, respectively. Thus, the animals with severe infarction could not survive for longer periods after ischemia, which might result in the reduction of infarct volume in *Sod1* +/−^{cep} animals at 96 hr after ischemia.

Hemisphere enlargement showed similar results as the infarct volume (Fig. 3C_2). The percentage of hemisphere enlargement was slightly increased at 8 hr after ischemia both in Wt and in *Sod1* +/−^{cep} mice (4.4 ± 1.1% vs 6.9 ± 0.9; $p = 0.63$) (Fig. 3C_2). The percentage of hemisphere enlargement highly increased in *Sod1* +/−^{cep} mice (22.7 ± 4.6%) and was significantly greater than that in Wt mice (8.9 ± 1.6; $p < 0.01$) (Fig. 3C_2). It gradually decreased in *Sod1* +/−^{cep} mice up to 96 hr after ischemia (48 hr, 18.8 ± 3.0%; 96 hr, 16.6 ± 4.3%), and no significant difference was seen, compared with Wt mice (48 hr, 10.4 ± 1.3%; 96 hr, 11.8 ± 1.9%) (Fig. 3C_2).

Table 3. Mortality of Wt and mutant mice after ischemia

Genotype	Number of dead/total animals (% mortality)		
	24 hr	48 hr	96 hr
Wt	2/18 (11.1)	2/7 (28.6)	5/9 (55.6)
Sod1+/−^{uc}	5/14 (35.7)	N/D	N/D
Sod1+/−^{cep}	5/21 (23.8)	4/8 (50.0)	7/11 (63.6)
Sod1−/−^{cep}	8/8 (100)	N/D	N/D

Each value represents number of dead mice/total mice and % mortality of each genotype and time course. N/D, Not determined.

Table 4. Neurological deficits of Wt and mutant mice at 24 hr after ischemia

Genotype	Neurological deficit scores[a]					
	0	1	2	3	4	Mean ± SEM[b]
Wt	3	7	5	0	1	1.31 ± 0.25
Sod1+/−^{uc}	0	1	2	3	3	2.89 ± 0.35**
Sod1+/−^{cep}	0	4	9	2	1	2.00 ± 0.20*

[a]Neurological deficit scores of 0–4: 0, no neurological deficit; 1, failed to extend right forepaw; 2, circled to the right; 3, fell to the right; 4, unable to walk spontaneously. Each value represents the number of animals in the respective scores.

[b]Each value represents mean ± SEM of neurological deficit scores; *$P < 0.05$, **$P < 0.01$, significantly different from Wt mice (Mann–Whitney *U* test).

Severity of infarction and brain swelling correlates the exacerbation of neurological deficits

We analyzed the correlation between infarct volume and hemisphere enlargement in individual animals at 24 hr after ischemia. Linear regression analysis (Fig. 4*A*) shows a positive correlation between the percentage of infarct volume and the percentage of hemisphere enlargement in Wt and *Sod1* +/− mice ($r = 0.80$). Individual data

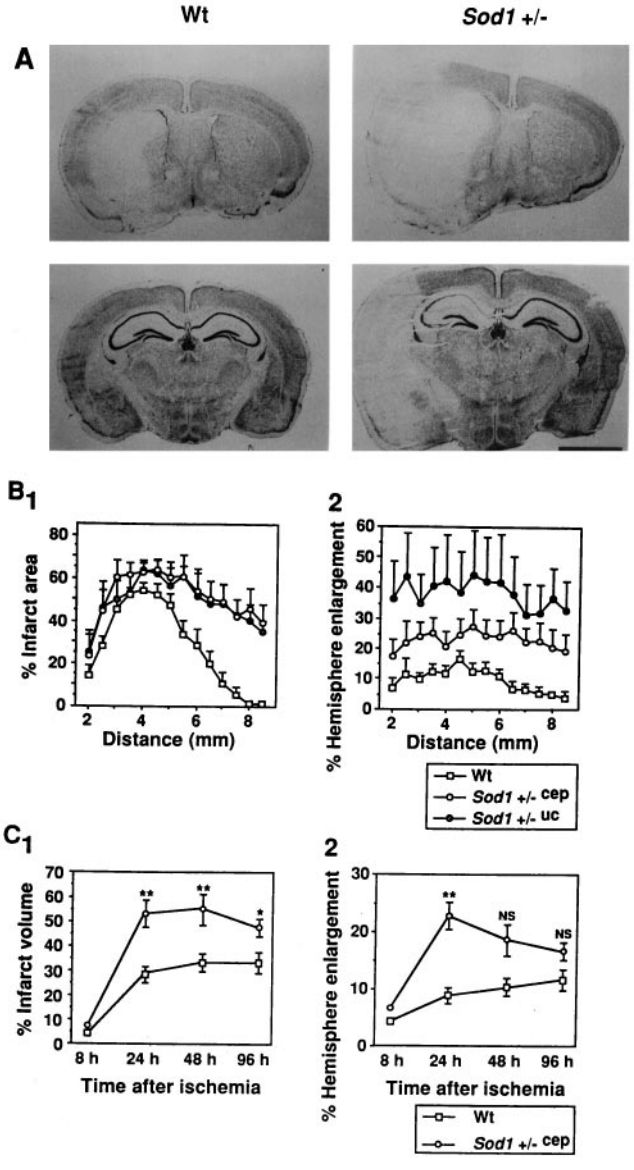

Figure 3. Histological analysis of Wt and *Sod1* +/− mice after ischemia. *A*, Representative low-magnification photograph of cresyl violet staining at 24 hr after 1 hr of MCA occlusion. The caudate putamen level at 3 mm from the anterior tip (*top*) and the hippocampal level at 6 mm from the anterior tip (*bottom*) are represented. Infarction is represented in the left hemisphere as a pale, stained area. The ischemic hemisphere is much more enlarged in *Sod1* +/− than in Wt mice. Note that hippocampal CA1 pyramidal neurons are also involved in the infarction in *Sod1* +/− mice. Scale bar, 2 mm. *B*, Distribution of infarction and hemisphere enlargement in the brain. B_1, Sequential changes of percentage of infarct area expressed as infarct area/ischemic hemisphere area × 100%. B_2, Sequential changes of percentage of hemisphere enlargement expressed as (ischemic hemisphere area − nonischemic hemisphere area)/nonischemic hemisphere area × 100%. *X*-axis shows the distance of the sections from the anterior tip of the brain. Data show mean ± SEM (n = 5–8). *C*, Temporal profile of infarct volume and hemisphere enlargement in the whole brain of Wt and *Sod1* +/−^{cep} mice. The percentages of total infarct volume (C_1) and percentages of total hemisphere enlargement (C_2) were calculated by the accumulation in consecutive brain sections and expressed in the same manner as in Figure 3*B*. Data show mean ± SEM (n = 4–8). *Asterisks* indicate a significant increase, compared with Wt mice ($^*p < 0.05$, $^{**}p < 0.01$), and *NS* indicates no significance between Wt and *Sod1* +/−^{cep} (Fisher's PLSD test).

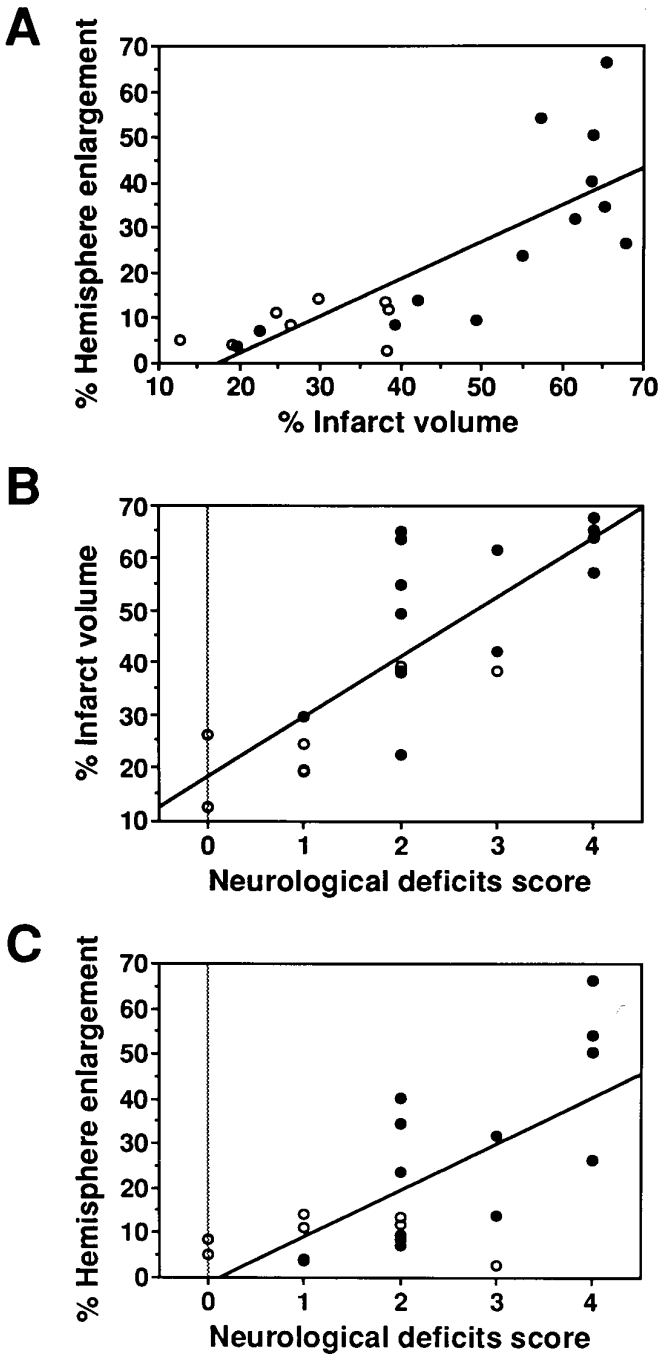

Figure 4. Correlation between histological findings and neurological deficits at 24 hr after ischemia. The results in individual Wt (*open circles*, n = 8) and *Sod1* +/− (*solid circles*, n = 13) mice are shown. *Lines* are linear regression that fit through the data points. *A*, Linear regression of percentage of infarct volume and percentage of hemisphere enlargement in Wt and *Sod1* +/− mice (r = 0.80). *B*, Linear regression of percentage of infarct volume on neurological deficit score in Wt and *Sod1* +/− mice (r = 0.79). *C*, Linear regression of percentage of hemisphere enlargement on neurological deficit score in Wt and *Sod1* +/− mice (r = 0.70).

plots also demonstrate the differences in the subpopulation of infarct volume and hemisphere enlargement between Wt and *Sod1* +/− mice. These results indicate that a decrease in the level of CuZn-SOD in *Sod1* +/− mice exacerbates both infarction and brain edema at 24 hr after 1 hr of MCA occlusion.

To examine the effects of the histological findings on the neu-

rological deficits, next we analyzed them by plotting variations of the percentage of infarct volume (Fig. 4*B*) or the percentage of hemisphere enlargement (Fig. 4*C*) versus neurological deficit scores in individual animals at 24 hr after ischemia. Linear regression analysis indicates that neurological deficits in individual animals were positively correlated with the percentage of infarct volume ($r = 0.79$) and the percentage of hemisphere enlargement ($r = 0.70$). These findings indicate that increased formation of infarction and brain edema causes exacerbation of neurological deficits in *Sod1* +/− mice.

Reduction of CuZn-SOD enhances neuronal apoptosis

To evaluate the role of oxygen-free radicals in the induction of apoptotic neuronal cell death in focal ischemic brain injury, we examined DNA fragmentation in the infarcted brain sections from Wt and *Sod1* +/− mice. As shown in Figure 5*B*, TUNEL staining does not label the normal neuronal cells in the noninfarct area. In contrast, two different patterns of staining were observed in the neuronal cells in the infarcted area (Fig. 5*D*,*F*). Some neuronal cells in the infarcted area are densely labeled in their nuclei using TUNEL staining, accompanied by small particles around the nuclei that resemble apoptotic bodies (Fig. 5*D*). These neuronal cells show cellular shrinkage and chromatin condensation in the nuclei using H & E staining (Fig. 5*C*). This cellular morphology is consistent with the apoptotic cell death process. Besides these typical apoptotic neuronal cells, slightly TUNEL-stained cells are also observed (Fig. 5*F*). These cells show diffuse nuclear staining by TUNEL and cellular swelling and nuclear lysis by H & E staining (Fig. 5*F*,*E*). This cellular morphology is consistent with necrosis. These results are consistent with those of previous reports, in which the coexistence of cells with either necrotic or apoptotic features is observed after focal cerebral ischemia and in which necrotic neurons are slightly labeled using TUNEL staining (Charriaut-Marlangue and Ben-Ari, 1995; Li et al., 1995b). The present study also confirms that apoptotic and necrotic features can be distinguished by the different patterns in TUNEL staining and that these differences in TUNEL staining are readily visualized by dark-field phase-contrast microscopy (Fig. 5*G*,*H*).

No differences were observed in the morphological features of apoptotic or necrotic neurons between Wt and *Sod1* +/− mice. However, the distribution and number of apoptotic neurons showed a notable difference between these groups. In Wt mice, apoptotic neurons were observed primarily at the margin of the inner boundary of the caudate putamen (Fig, 6*A*). In other lesions of the infarction (i.e., center of the caudate putamen, the cortical penumbra, and the piriform cortex), the main population of the cells showed necrotic features (Fig, 6*A*,*C*,*E*). In contrast, in *Sod1* +/− mice, an increased number of apoptotic neurons were observed in the caudate putamen (Fig. 6*B*), and the main population of the cells showed apoptotic features in the cortical penumbra (Fig. 6*D*) and the piriform cortex (Fig. 6*F*).

To quantify the apoptotic neurons, we assessed temporal resolution of TUNEL-positive cells between Wt and *Sod1* +/− mice. The number of apoptotic neurons was counted at 8, 24, 48, and 96 hr after 1 hr of MCA occlusion in the inner boundary of the caudate putamen, the center of the caudate putamen, the cortical penumbra, and the piriform cortex, respectively. As illustrated in Figure 7, apoptotic neurons were scarce at 8 hr after ischemia. They were remarkably increased at 24–48 hr and decreased at 96 hr after ischemia, both in Wt and in *Sod1* +/− mice. These results are consistent with those of previous reports for the temporal profile of apoptotic neurons after focal cerebral ischemia in the rat (Li et al., 1995a). Although there are no differences in the pattern of temporal profile in the apoptotic neurons between Wt and *Sod1* +/− mice, apoptotic cell numbers are increased significantly in *Sod1* +/− than in Wt mice at 24 and 48 hr after ischemia ($p < 0.05$–0.01) (Fig. 7). These experiments demonstrate that in ischemic-reperfusion injury, apoptotic neuronal cell death is increased in *Sod1* +/− mice. These findings are consistent with the

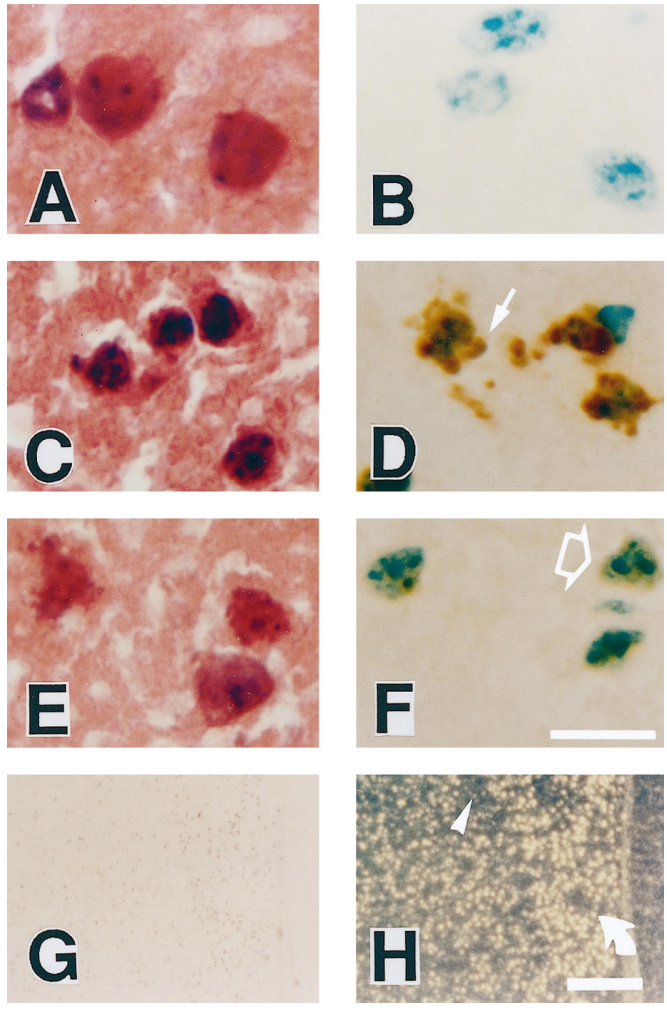

Figure 5. Representative findings of TUNEL staining in Wt mice at 24 hr after ischemia. High magnification of neuronal cells in the caudate putamen with H & E staining (*A*, *C*, *E*) and TUNEL staining with methyl green counter staining (*B*, *D*, *F*). *A*, *B*, The nuclear and cellular morphology of the neurons in the nonischemic caudate putamen is typical of normal neurons with smooth nuclear membrane and uniform chromatin formation (*A*). TUNEL staining does not label normal neuronal cells (*B*). *C*, *D*, Representative morphology of the cells in the marginal zone of the infarction, which shows apoptotic features such as cell shrinkage and chromatin condensation in the nuclei (*C*). Apoptotic neuronal cells in the marginal zone are recognized with TUNEL staining with markedly labeled small particles, called "apoptotic bodies," around the nuclei (*D*, *arrow*). *E*, *F*, Representative morphology of the cells in the infarction, which shows necrotic features such as cellular swelling (pale color on eosinophilic staining) and irregularly shaped nuclei (*E*). These neuronal cells are slightly labeled with TUNEL staining in the nuclei (F, *open arrow*). *G*, *H*, Lower magnification of TUNEL staining by bright-field (*G*) and dark-field (*H*) phase-contrast microscopy. Two patterns of the staining quality are emphasized in the dark-field phase-contrast photomicrographs: apoptotic neurons with dense TUNEL labeling as *bright yellow spots* (*H*, *rotated arrow*) and necrotic neurons with slight TUNEL labeling as faint, small, yellow spots (*H*, *arrowhead*). Scale bars: *A–F*, 20 μm; *G*, *H*, 200 μm.

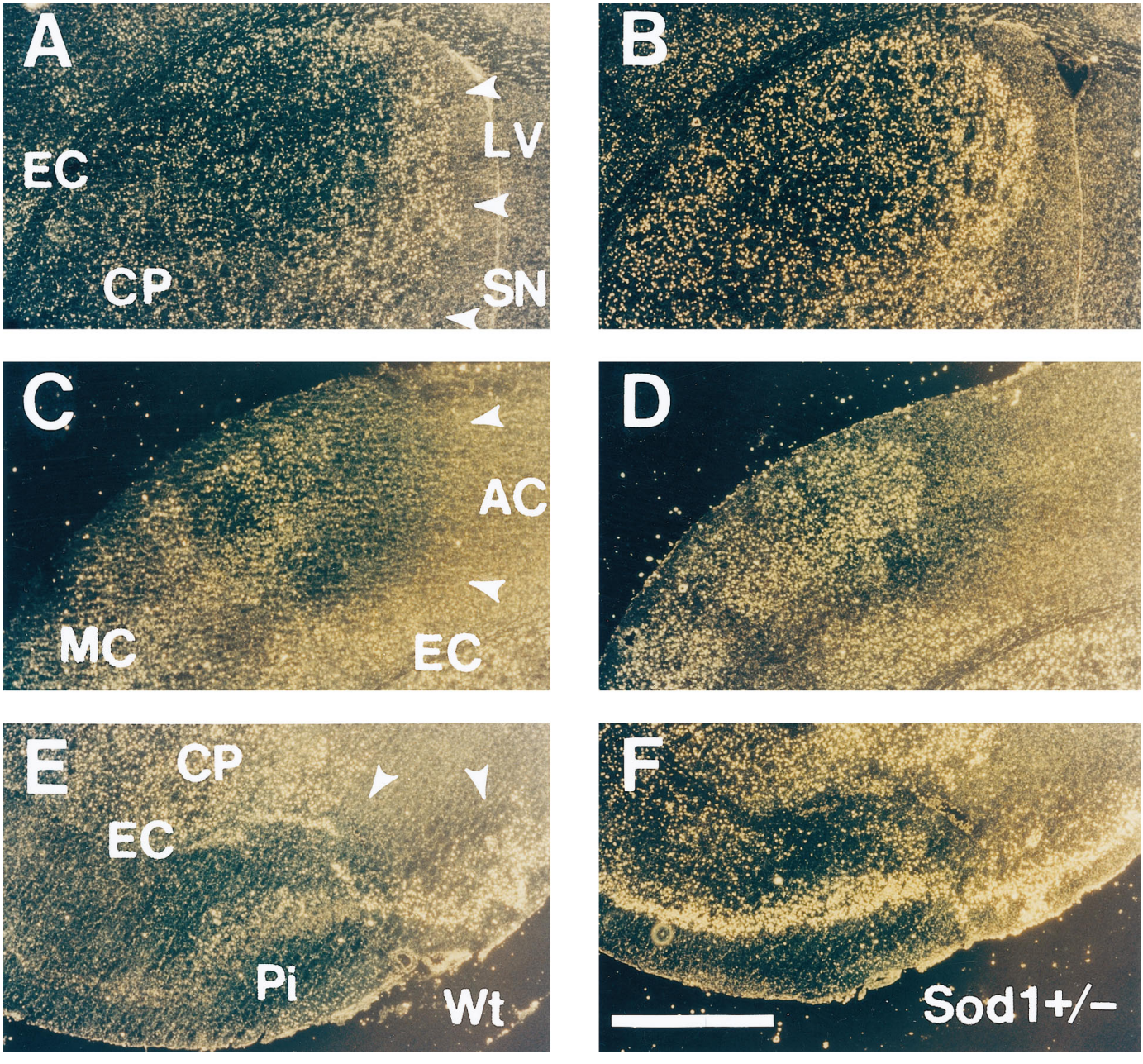

Figure 6. Distribution of TUNEL-positive neurons in Wt and *Sod1* +/− mice. Representative dark-field phase-contrast photographs of TUNEL staining in Wt (*A*, *C*, *E*) and heterozygous mutant (*B*, *D*, *F*) mice at 24 hr after 1 hr of MCA occlusion. Normal, noninfarcted area gives yellow reticular background, and infarct area is defined as dark area (*A*, *C*, *E*, *arrowheads*). In the infarcted area, *bright yellow* spots representing apoptotic neurons with dense TUNEL labeling and *faint yellow* spots representing necrotic neurons with slight TUNEL labeling are observed. In the caudate putamen, the apoptotic neurons are located primarily at the margin of the inner boundary, and the center of the caudate putamen was occupied with necrotic neurons in Wt mice (*A*). In contrast, apoptotic neurons were increased in the margin of the inner boundary and extend to the center of the caudate putamen in *Sod1* +/− mice (*B*). In the cortical penumbra, an increased number of apoptotic neurons is observed in *Sod1* +/− mice (*D*), compared with Wt mice (*C*). In the piriform cortex, apoptotic neurons are scarce in Wt mice (*E*), whereas almost all neurons show apoptotic features in *Sod1* +/− mice (*F*). *LV*, Lateral ventricle; *CP*, caudate putamen; *EC*, external capsule; *SN*, septal nucleus; *AC*, territory of anterior cerebral artery; *MC*, territory of middle cerebral artery; *Pi*, piriform cortex. Scale bar, 500 μm.

idea that oxidative stress mediates apoptotic neuronal cell death (Kane et al., 1993; Troy and Shelanski, 1994; Greenlund et al., 1995). Here we have extended this concept to the role of oxygen-free radicals in apoptotic neuronal cell death in focal ischemic brain injury.

DISCUSSION

Targeted disruption of the *Sod1* gene results in the partial or complete loss of CuZn-SOD activity in mutant mice. In this study, we present data that show that the formation of brain edema and neuronal cell injury, including apoptotic neuronal cell death, is exacerbated in mutant mice after focal cerebral ischemia. Because phenotypic abnormalities are not seen in the mutant mice under normal physiological conditions, these findings are consistent with the hypothesis that an increased level of oxygen-free radicals, especially O_2^-, mediates these pathologies in the mutant mice after focal cerebral ischemia.

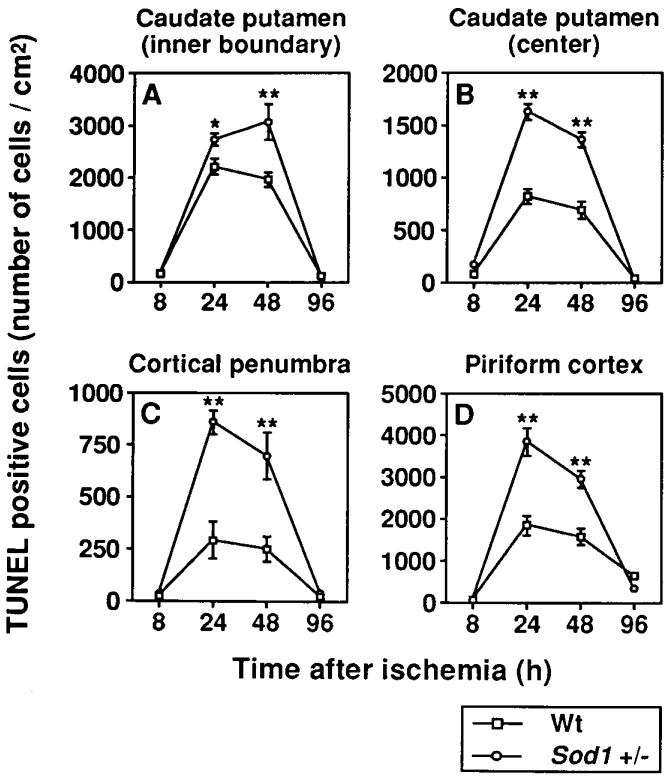

Figure 7. Temporal profile of TUNEL-positive neurons in Wt and *Sod1* +/− mice. Apoptotic neuronal cells were counted at 8, 24, 48, and 96 hr after 1 hr of MCA occlusion in the inner boundary of the caudate putamen (*A*), the center of the caudate putamen (*B*), the cortical penumbra (*C*), and the piriform cortex (*D*). Data are expressed as cells/mm^2 (for details, see Results). Data represent mean ± SEM ($n = 4$). *Asterisks* indicate a significant increase, compared with Wt mice ($^*p < 0.05$, $^{**}p < 0.01$; Fisher's PLSD test).

The present study demonstrated high mortality and exacerbated neurological deficits in mutant mice after focal cerebral ischemia. The mechanisms underlying exacerbated mortality and neurological deficits in mutant mice are unclear at present. However, in ischemic brain injury, brain edema is known to be an important factor for the acute phase of mortality because of the development of severe brain swelling and herniation. Our results indicate that BBB disruption occurs unusually early in mutant mice, with the amount of Evans blue leakage being dependent on the degree of decreased CuZn-SOD activity. In addition, at later time points, mutant mice showed severe brain swelling that was correlated to neurological deficits. This severe brain edema is suggested to be the primary factor causing the exacerbation of mortality and neurological deficits in the mutant animals. The BBB, which is composed of endothelial cells, is intact several hours after ischemia (Menzies et al., 1993), suggesting that endothelial cells are relatively resistant to ischemic injury (Brightman, 1992). Because the endothelial cells are a major cellular source of O_2^- through high levels of xanthine oxidase (Betz, 1985; Terada et al., 1991), our findings suggest that O_2^- may contribute to the ischemic vulnerability of endothelial cells in mutant mice. O_2^- is known to produce highly toxic hydroxyl radicals through two distinct pathways; the first is reaction with H_2O_2 through the Haber–Weiss reaction; the second is peroxynitrite self-decomposition through a reaction with nitric oxide. However, the former pathway appears unlikely in the mutant mice, because O_2^- is hardly converted to H_2O_2 in cytosol, especially in the *Sod1* −/− mutants, because of the lack of CuZn-SOD activity. The latter pathway more likely explains the phenomenon in the mutants, because endothelial cells are an abundant source of nitric oxide from their constitutive nitric oxide synthase. Consistent with this inference is recent evidence suggesting that the constitutive endothelial nitric oxide synthase is activated after focal cerebral ischemia and reperfusion (Nagafuji et al., 1995).

It is known that exogenously supplied SOD improves the histological outcome in ischemic animals by increasing the CBF (Cerchiari et al., 1987). However, our previous reports demonstrated that endogenously increased CuZn-SOD activity in transgenic mice has no effect on CBF during and after ischemia (Chan et al., 1993; Yang et al., 1994; Kondo et al., 1996). The present study also confirms that a decreased level of CuZn-SOD in mutant mice does not affect the residual CBF during ischemia. Recently, Barone et al. (1993) reported a significant difference between mouse strains in their sensitivity to focal ischemia that was related to the structural and functional differences in the potency of the circle of Willis. Although the functional vascular anatomy was not examined in the present study, a similar level of CBF decreases during ischemia in Wt and mutant animals clearly suggests that functional vascular anatomy does not play a role in the outcomes after focal cerebral ischemia. In addition, two different mutant mouse strains (*Sod1* +/−^{uc} and *Sod1* +/−^{cep}) with different genetic backgrounds showed almost the same distribution and volume of infarction, which were remarkably different from those in Wt mice. These results again suggest that because of the decreased level of CuZn-SOD activity, the severity of the infarction in the mutant mice is related to the biochemical reaction of oxygen-free radicals.

The effects of oxidative stress on the biochemical mechanisms in focal ischemic brain injury have been shown in a variety of experimental studies. In the present study, sequential changes in the infarct area demonstrated that infarction was extended to the posterior side of the cortex in heterozygous mutant mice. This finding suggests that the decreased level of CuZn-SOD is related to or accelerates the damage of the neuronal cells located in the cortical penumbra area. One important metabolic event in the penumbra area is the depolarization that causes Ca^{2+} overload by excitatory amino acids (Simon and Shiraishi, 1989). A recent study provides direct evidence that excitotoxic neuronal cell death requires O_2^- generation in cultured cortical neurons (Patel et al., 1996), suggesting that the excitotoxic events may contribute to the formation of infarction through a high level of O_2^- in the penumbra area in the mutant mice. The present study also demonstrates that hippocampal CA1 neurons are involved in the infarction in mutant mice. A variety of experimental models of global cerebral ischemia have demonstrated that CA1 hippocampal pyramidal neurons are the cells most vulnerable to ischemic injury (Pulsinelli and Brierley, 1979; Kirino, 1982), in which abundant NMDA receptors are expressed (Monaghan and Cotman, 1985), suggesting that activation of NMDA receptors contributes to CA1 vulnerability. These findings again support the possibility that excitotoxic events may contribute to neuronal cell injury in the mutant mice.

The appearance of apoptotic neuronal cell death in focal ischemic brain injury has recently been observed. DNA laddering (a biochemical hallmark of apoptosis) after MCA occlusion in the rat is associated with increased intranucleosomal endonuclease activity (Tominaga et al., 1993). Recent morphological studies with TUNEL staining demonstrate that the inner boundary zone

of the caudate putamen is vulnerable to apoptotic neuronal cell death after focal cerebral ischemia (Li et al., 1995b; Charriaut-Marlangue et al., 1996), and the number of apoptotic neurons was maximized at 24–48 hr after ischemia (Li et al., 1995a). Our results in Wt mice are consistent with these previous reports. The present study provides a new perspective that whereas a small number of neurons in the core of the ischemia show apoptotic neuronal cell death in Wt mice, the number is increased significantly in the mutant mice. Because neurons in the core of the ischemic region rapidly die, it is difficult to explain this phenomenon. Recent studies have demonstrated that a neurotoxic dose of glutamate induced acute necrosis in a subpopulation of cerebellar granule cells during and immediately after exposure, whereas the remaining neurons died from delayed-onset apoptosis (Ankarcrona et al., 1995). Furthermore, excitotoxic animal models suggest that apoptotic and necrotic mechanisms of neuronal death may occur simultaneously within individual dying cells in the injured brain (Portera-Cailliau et al., 1995). These findings are likely to explain tissue injury such as in focal ischemic brain injury, in which cells with either necrotic or apoptotic features coexist. Thus, even in the core of the infarction, some neuronal subpopulations die rapidly via the necrotic process, and the remaining neuronal cells may die gradually by the apoptotic process, which could be enhanced by a decreased level of CuZn-SOD in the mutant mice.

More importantly, heterozygous mutant mice demonstrate significantly increased apoptotic neuronal cell death in the cortical penumbra and piriform cortex, suggesting that oxygen-free radicals, in particular O_2^-, are important factors for inducing apoptotic neuronal cell death in focal ischemic brain injury. These results are consistent with recent studies in which CuZn-SOD, as well as BCL-2 (recently shown to have antioxidant properties), has been found to delay or prevent neuronal apoptosis by growth factor deprivation in culture (Hockenbery et al., 1993; Kane et al., 1993). In addition, Araki et al. (1992) demonstrated that SOD attenuated increases in intracellular Ca^{2+} concentration after MCA occlusion, suggesting that a decreased level of CuZn-SOD in the mutant mice induces Ca^{2+} overload, subsequently leading to apoptosis. A recent study has demonstrated that mild focal ischemia causes delayed infarction, related to the appearance of apoptotic neurons (Du et al., 1996), suggesting the important role of apoptotic neuronal cell death in the development of ischemic brain injury. This finding supports our hypothesis that CuZn-SOD-related modulation of neuronal viability is related to the inhibition of apoptotic neuronal cell death after focal cerebral ischemia and reperfusion.

We have presented data showing that mutant mice exhibit exacerbation of ischemic brain injury through early, severe BBB disruption and subsequent infarction with increased apoptotic neuronal cell death. The early BBB breakdown suggests that the vulnerability of the endothelial cells makes them a target for early oxygen-free radical damage in the mutant mice. Differences in cellular distribution of necrosis and apoptosis in heterozygous mutants suggest that excitotoxic events play a critical role in brain injury induced by oxidative stress after focal cerebral ischemia. Current data are consistent with the hypothesis that a series of biochemical events involving the generation of O_2^-, perhaps peroxynitrite formation and Ca^{2+} overload, is involved. This schema, although it is still incomplete, provides a framework for additional mechanistic studies.

REFERENCES

Ankarcrona M, Dypbukt JM, Bonfoco E, Zhivotovsky B, Orrenius S, Lipton SA, Nicotera P (1995) Glutamate-induced neuronal death: a succession of necrosis or apoptosis depending on mitochondrial function. Neuron 15:961–973.

Araki N, Greenberg JH, Uematsu D, Sladky JT, Reivich M (1992) Effect of superoxide dismutase on intracellular calcium in stroke. J Cereb Blood Flow Metab 12:43–52.

Barone FC, Knudsen DJ, Nelson AH, Feuerstein GZ, Willette RN (1993) Mouse strain differences in susceptibility to cerebral ischemia are related to cerebral vascular anatomy. J Cereb Blood Flow Metab 13:683–692.

Betz AL (1985) Identification of hypoxanthine transport and xanthine oxidase activity in brain capillaries. J Neurochem 44:574–579.

Brightman MW (1992) Ultrastructure of brain endothelium. In: Physiology and pharmacology of the blood–brain barrier (Bradbury MWB, ed), pp 1–19. Berlin: Springer.

Cerchiari EL, Hoel TM, Safar P, Sclabassi RJ (1987) Protective effects of combined superoxide dismutase and deferoxamine on recovery of cerebral blood flow and function after cardiac arrest in dogs. Stroke 18:869–878.

Chan PH (1994) Oxygen radicals in focal cerebral ischemia. Brain Pathol 4:59–65.

Chan PH, Fishman RA, Schmidley JW, Chen SF (1984) Release of polyunsaturated fatty acids from phospholipids and alteration of brain membrane integrity by oxygen-derived free radicals. J Neurosci Res 12:595–605.

Chan PH, Yang GY, Chen SF, Carlson E, Epstein CJ (1991) Cold-induced brain edema and infarction are reduced in transgenic mice overexpressing CuZn-superoxide dismutase. Ann Neurol 29:482–486.

Chan PH, Kamii H, Yang G, Gafni J, Epstein CJ, Carlson E, Reola L (1993) Brain infarction is not reduced in SOD-1 transgenic mice after a permanent focal cerebral ischemia. NeuroReport 5:293–296.

Charriaut-Marlangue C, Ben-Ari Y (1995) A cautionary note on the use of the TUNEL stain to determine apoptosis. NeuroReport 7:61–64.

Charriaut-Marlangue C, Margaill I, Represa A, Popovici T, Plotkine M, Ben-Ari Y (1996) Apoptosis and necrosis after reversible focal ischemia: an *in situ* DNA fragmentation analysis. J Cereb Blood Flow Metab 16:186–194.

Choi DW (1988) Glutamate neurotoxicity and diseases of the nervous system. Neuron 1:623–634.

Du C, Hu R, Csernansky CA, Hsu CY, Choi DW (1996) Very delayed infarction after mild focal cerebral ischemia: a role for apoptosis? J Cereb Blood Flow Metab 16:195–201.

Epstein CJ, Avraham KB, Lovett M, Smith S, Elroy SO, Rotman G, Bry C, Groner Y (1987) Transgenic mice with increased Cu/Zn-superoxide dismutase activity: animal model of dosage effects in Down syndrome. Proc Natl Acad Sci USA 84:8044–8048.

Fridovich I (1986) Biological effects of the superoxide radical. Arch Biochem Biophys 247:1–11.

Gaudet RJ, Levine L (1979) Transient cerebral ischemia and brain prostaglandins. Biochem Biophys Res Commun 86:893–901.

Gavrieli Y, Sherman Y, Ben-Sasson SA (1992) Identification of programmed cell death *in situ* via specific labeling of nuclear DNA fragmentation. J Cell Biol 119:493–501.

Greenlund LJS, Deckwerth TL, Johnson Jr EM (1995) Superoxide dismutase delays neuronal apoptosis: a role for reactive oxygen species in programmed neuronal death. Neuron 14:303–315.

Hockenbery DM, Oltvai ZN, Yin XM, Milliman CL, Korsmeyer SJ (1993) Bcl-2 functions in an antioxidant pathway to prevent apoptosis. Cell 75:241–251.

Kamii H, Kinouchi H, Sharp FR, Koistinaho J, Epstein CJ, Chan PH (1994) Prolonged expression of hsp70 mRNA following transient focal cerebral ischemia in transgenic mice overexpressing CuZn-superoxide dismutase. J Cereb Blood Flow Metab 14:478–486.

Kane DJ, Sarafian TA, Anton R, Hahn H, Butler Gralla E, Selverstone Valentine J, Örd T, Bredesen DE (1993) Bcl-2 inhibition of neuronal death: decreased generation of reactive oxygen species. Science 262:1274–1277.

Kinouchi H, Epstein CJ, Mizui T, Carlson E, Chen SF, Chan PH (1991) Attenuation of focal cerebral ischemic injury in transgenic mice overexpressing CuZn superoxide dismutase. Proc Natl Acad Sci USA 88:11158–11162.

Kirino T (1982) Delayed neuronal death in the gerbil hippocampus following ischemia. Brain Res 239:57–69.

Kondo T, Murakami K, Honkaniemi J, Sharp FR, Epstein CJ, Chan PH (1996) Expression of hsp70 mRNA is induced in the brain of transgenic mice overexpressing human CuZn-superoxide dismutase following transient global cerebral ischemia. Brain Res 737:321–326.

Kure S, Tominaga T, Yoshimoto T, Tada K, Narisawa K (1991) Glutamate triggers internucleosomal DNA cleavage in neuronal cells. Biochem Biophys Res Commun 179:39–45.

Li Y, Chopp M, Jiang N, Yao F, Zaloga C (1995a) Temporal profile of *in situ* DNA fragmentation after transient middle cerebral artery occlusion in the rat. J Cereb Blood Flow Metab 15:389–397.

Li Y, Chopp M, Jiang N, Zaloga C (1995b) *In situ* detection of DNA fragmentation after focal cerebral ischemia in mice. Brain Res Mol Brain Res 28:164–168.

Linnik MD, Zobrist RH, Hatfield MD (1993) Evidence supporting a role for programmed cell death in focal cerebral ischemia in rats. Stroke 24:2002–2009.

Liu TH, Beckman JS, Freeman BA, Hogan EL, Hsu CY (1989) Polyethylene glycol-conjugated superoxide dismutase and catalase reduce ischemic brain injury. Am J Physiol 256:H589–H593.

MacManus JP, Hill IE, Huang ZG, Rasquinha I, Xue D, Buchan AM (1994) DNA damage consistent with apoptosis in transient focal ischaemic neocortex. NeuroReport 5:493–496.

McCord JM (1985) Oxygen-derived free radicals in postischemic tissue injury. N Engl J Med 312:159–163.

McCord JM, Fridovich I (1969) Superoxide dismutase: an enzymic function for erythrocuprein (hemocuprein). J Biol Chem 244:6049–6055.

Menzies SA, Betz AL, Hoff JT (1993) Contributions of ions and albumin to the formation and resolution of ischemic brain edema. J Neurosurg 78:257–266.

Monaghan DT, Cotman CW (1985) Distribution of *N*-methyl-D-aspartate-sensitive L-[^{3}H]glutamate-binding sites in rat brain. J Neurosci 5:2909–2919.

Nagafuji T, Sugiyama M, Matsui T, Muto A, Naito S (1995) Nitric oxide synthase in cerebral ischemia. Mol Chem Neuropathol 26:107–157.

Orrenius S, Burkitt MJ, Kass GE, Dypbukt JM, Nicotera P (1992) Calcium ions and oxidative cell injury. Ann Neurol 32[Suppl]:S33–S42.

Patel M, Day BJ, Crapo JD, Fridovich I, McNamara JO (1996) Requirement for superoxide in excitotoxic cell death. Neuron 16:345–355.

Pazdernik TL, Layton M, Nelson SR, Samson FE (1992) The osmotic/calcium stress theory of brain damage: are free radicals involved? Neurochem Res 17:11–21.

Portera-Cailliau C, Hedreen JC, Price DL, Koliatsos VE (1995) Evidence for apoptotic cell death in Huntington disease and excitotoxic animal models. J Neurosci 15:3775–3787.

Pulsinelli WA, Brierley JB (1979) A new model of bilateral hemispheric ischemia in the unanesthetized rat. Stroke 10:267–272.

Reaume AG, Elliott JL, Hoffman EK, Kowall NW, Ferrante RJ, Siwek DF, Wilcox IM, Flood DG, Beal MF, Brown RHJ, Scott RW, Snider WD (1996) Motor neurons in Cu/Zn superoxide dismutase-deficient mice develop normally but exhibit enhanced cell death after axonal injury. Nat Genet 13:43–47.

Saugstad OD, Aasen AO (1980) Plasma hypoxanthine concentration in pigs a prognostic aid in hypoxia. Eur Surg Res 12:123–129.

Shukla A, Shukla R, Dikshit M, Srimal RC (1993) Alterations in free radical scavenging mechanisms following blood–brain barrier disruption. Free Radic Biol Med 15:97–100.

Siesjö BK (1984) Cerebral circulation and metabolism. J Neurosurg 60:883–908.

Simon R, Shiraishi K (1989) *N*-methyl-D-aspartate antagonist reduces stroke size and regional glucose metabolism. Ann Neurol 27:606–611.

Terada LS, Willingham IR, Rosandich ME, Leff JA, Kindt GW, Repine JE (1991) Generation of superoxide anion by brain endothelial cell xanthine oxidase. J Cell Physiol 148:191–196.

Tominaga T, Kure S, Narisawa K, Yoshimoto T (1993) Endonuclease activation following focal ischemic injury in the rat brain. Brain Res 608:21–26.

Troy CM, Shelanski ML (1994) Down-regulation of copper/zinc superoxide dismutase causes apoptotic death in PC12 neuronal cells. Proc Natl Acad Sci USA 91:6384–6387.

Yang G, Chan PH, Chen J, Carlson E, Chen SF, Weinstein P, Epstein CJ, Kamii H (1994) Human copper-zinc superoxide dismutase transgenic mice are highly resistant to reperfusion injury after focal cerebral ischemia. Stroke 25:165–170.